Ultra-microporous adsorbents prepared from vine shoots-derived biochar with high CO_2 uptake and CO_2/N_2 selectivity.

Joan J. Manyà[a,b,*], Belén González[a,b], Manuel Azuara[b,c], Gabriel Arner[b]

[a] *Aragón Institute of Engineering Research (I3A),* [b] *Technological College of Huesca,* and [c] *Institute of Nanoscience of Aragón (INA), University of Zaragoza, crta. Cuarte s/n, Huesca E-22071, Spain*

* Corresponding author.

E-mail: joanjoma@unizar.es (Joan J. Manyà).

Keywords

Postcombustion CO_2 capture; Carbon-based adsorbents; Biochar; Vine shoots; Selectivity CO_2/N_2

ABSTRACT

There is a growing interest in developing renewable biomass-based adsorbents to be used in numerous applications, including CO_2 capture in postcombustion conditions. In the present study, several activated carbons (ACs) were produced from vine shoots-derived biochar through both physical and chemical activation using CO_2 and KOH, respectively. The performance of these ACs was tested in terms of CO_2 uptake capacity at an absolute pressure of 15 kPa and at different temperatures (0, 25, and 75 °C), apparent selectivity towards CO_2 over N_2, and isosteric heat of adsorption. At 25 °C, the chemically ACs with KOH impregnation exhibited the highest CO_2 adsorption capacity, which was similar or even higher than those recently reported for a number of carbon-based adsorbents. However, the AC prepared through physical activation with CO_2 at 800 °C and a soaking time of 1 h appears as the most promising adsorbent analyzed here, due to its higher CO_2 uptake capacity and adsorption rate at relatively high temperature (75 °C), its relatively high selectivity at this temperature, and its apparently low energy demand for regeneration. Given that physical activation with CO_2 is more feasible at industrial scale than chemical activation using corrosive alkalis, the results reported here are encouraging for further development of vine shoots-derived adsorbents.

1. Introduction

Anthropogenic CO_2 emissions from the burning of fossil fuels have been considered as the major contributor for global warming. In the near future, fossil fuels will be continuing as a predominant energy source. Thus, research aimed at reducing CO_2 release is imperative. In this context, carbon capture and storage (CCS) appears as one of the most promising solutions [1]. Chemical absorption using aqueous amine-solutions is a mature technology for postcombustion capture. However, this technology has several drawbacks, being the most important the energy-intensive regeneration step [2]. Compared with liquid amine-based absorption, CO_2 capture via adsorption processes is a more promising alternative because of its low energy consumption during regeneration and low capital investment costs [3].

Until now, solid adsorbents as carbons [2], zeolites [4], metal oxihydroxide-biochar composites [5], porous polymers [6], and metal-organic frameworks (MOFs) [7] have been tested for CO_2 adsorption. Among them, carbonaceous adsorbents are probably the most interesting materials in view of their relatively low cost, low energy requirement for regeneration, high tolerance to moisture in the flue gas, and high chemical and mechanical stability [1]. From a sustainability point of view, when the precursors used to prepare porous carbons are lignocellulosic materials (or biochar produced from them), the attractiveness of these materials is further enhanced.

For postcombustion CO_2 capture, suitable adsorbents must meet the following requirements [8,9]: (i) high CO_2 adsorption capacity at low CO_2 partial pressures (5–15 kPa), (ii) high selectivity towards CO_2 over N_2, (iii) low or moderate heat of adsorption, and (iv) fast adsorption kinetics. Numerous studies were focused on producing activated carbons (ACs) from different biomass precursors; for instance: olive stones [10], almond shells [10], coconut shell [9], eucalyptus wood [11] and sawdust [12], pinewood sawdust [13], wheat straw [13], grass cuttings [8], poultry litter

[13], and horse manure [8]. The preparation of ACs usually involves two steps [2]: (1) converting biomass into biochar or hydrochar (through pyrolysis and hydrothermal carbonization, respectively) and (2) activating the produced char at high temperature conditions (600–900 °C) either physically (by steam, CO_2, or O_2) or chemically (with KOH or H_3PO_4) to develop a porous structure [13]. Obviously, the physicochemical properties of the final product will depend on the nature of the precursor (properties of biomass materials are highly variable and heterogeneous), carbonization conditions, activation agents, and activation conditions [13].

Regarding the structural properties of ACs, Hao et al. [8] highlighted the key role played by the ultra-micropores (pore size < 0.7 nm) during CO_2 adsorption. For physically activated carbons from hydrochar precursors, Hao et al. [8] observed that the large volume of ultra-micropores, instead of the specific surface area, was the main parameter affecting the CO_2 adsorption capacity (a highest value of 1.45 mmol g^{-1} at 0 °C and 10 kPa was reported) as well as the selectivity CO_2/N_2. Li et al. [14] reported excellent CO_2 adsorption capacities (1.9–2.1 mmol g^{-1} at 0 °C and 10 kPa) for ACs prepared by KOH activation of rice husk-derived pyrogenic char. Li et al. [14] also attributed this result to the large volume of ultra-micropores (0.15 cm^3 g^{-1}) measured for their ACs.

The CO_2-over-N_2 selectivity of a porous sorbent can mainly be explained by thermodynamic and kinetic contributions [15]. Given that the molecule of CO_2 has a higher quadrupole moment (-13.7×10^{-24} cm^2) than that of N_2 (-4.9×10^{-26} cm^2), the interaction of CO_2 with the electrical field gradients of the sorbent can be higher than that of N_2. From the kinetic perspective, the effective kinetic diameter within porous solids of CO_2 is a little bit smaller than that of N_2 (0.33 nm and 0.36 nm, respectively). Thus, the diffusion of CO_2 through the ultra-micropores of sorbents can be faster than that of N_2, especially when the adsorbent has relatively uniform pores with sizes approaching the effective kinetic diameter of N_2 [16].

Recently, Chen et al. [17] measured high CO_2 adsorption capacities (1.6–1.9 mmol g^{-1} at 0 °C and 10 kPa) for N-doped carbon adsorbents produced by KOH activation of coconut shells-derived biochar. Modifying the sorbent surface with nitrogen functional groups can lead to an enhancement of the adsorption capacity of acidic gases such as CO_2 [11,17]. N-doped porous carbons can be prepared by two methods: (1) chemical or physical activation of a mixture of N-containing compounds (such as urea [17] or ammonium carbonate [18]) and the carbonized biomass precursor, and (2) physical activation with N-containing gases (e.g., ammonia [11]). Nevertheless, the effect of N-doping on the CO_2 uptake is unclear. In fact, a negligible effect has been reported in some earlier studies [18–20], indicating that the CO_2 adsorption behavior can predominantly be controlled by the volume of ultra-micropores (in terms of CO_2 adsorption capacity and CO_2-over-N_2 kinetic selectivity) and the surface chemistry (in terms of CO_2-over-N_2 thermodynamic selectivity) [13].

Vine shoots is a pruning residue widely produced in vineyards. Almost 1000 kha were used for vine cultivation in Spain in 2016 [21]. Assuming a waste yield of 1.9 ton ha^{-1} (dry basis), around 1.9 10^6 tons of vine shoots are harvested per year in Spain [22]. The disposal of vine shoots usually consists of shredding and burying them during harvest to return the organic matter to soil. Nevertheless, this practice can lead to negative effects in the health of vineyards due to the potential risk of increased inoculum [22]. For this reason, there is a growing interest in producing biochar from this waste as a means to improve soil quality and sequester carbon. In this context, developing biomass-derived carbon materials for alternative uses other than soil amendment (e.g., adsorbents for CO_2 capture) can increase the value of biomass and products and generate new technologies for biomass upcycling. There are some previous studies available in the literature concerning the production of ACs from vine shoots by physical and chemical activation methods [23–25].

However, the ability of vine shoots-derived ACs to capture CO_2 from flue gas has not been measured yet.

The specific aim of this study was to prepare several ACs from vine shoots-derived biochar and measure their performance as CO_2 adsorbents in postcombustion conditions. Different activation processes, including physical activation with CO_2 and chemical activation with KOH, were used in order to determine the effects of treatment on the properties and performance of produced ACs. The CO_2 adsorption capacities for the produced ACs were measured at 0, 25, and 75 °C and at a CO_2 pressure of 15 kPa (the usual highest value in postcombustion CO_2 capture), whereas the apparent selectivities CO_2/N_2 were measured at 25 and 75 °C in an atmospheric thermogravimetric analyzer under pure CO_2 or N_2 environment. Special attention was focused on assessing the relationships between the key structural properties of ACs (e.g., volume of ultra-micropores) and their performance in terms of CO_2 uptake and selectivity CO_2/N_2.

2. Experimental section

2.1. Vine shoots-derived biochar

The vine shoots used in the present study were supplied by a winery from the Denomination of Origin Somontano (Spain). Results from proximate and elemental analyses as well as ash composition for vine shoots are given in Table S1 of Supplementary Data. The as-received vine shoots (with particle sizes in the range of 0.1–1.0 cm diameter and 1.0–3.5 cm long) were pyrolyzed in a packed-bed reactor at a peak temperature of 600 °C and at an absolute pressure of 0.1 MPa. The details of the pyrolysis device and experimental procedure have been reported elsewhere [22,26]. Briefly, approximately 400 g of vine shots were heated at 0.1 MPa at an average heating rate of 5 $°C \cdot min^{-1}$ to the peak temperature (600 °C) with a soaking time of 60 min at this

temperature. A nitrogen mass flow rate of 600 mL min^{-1} (at STP conditions) was passed through the reactor (theoretical mean residence time of N_2 = 116 s).

2.2. Activation

The produced vine-shoots derived biochars (which were milled and sieved to a particle size distribution of 0.6–1.6 mm) were activated by both physical and chemical methods. For physical activation, 10 g of biochar was heated at 10 °C min^{-1} to 800 °C under a steady flow of CO_2 (100 mL min^{-1} STP) in a vertical fixed-bed quartz reactor (25 mm ID) at atmospheric pressure. The activation temperature of 800 °C was chosen according to earlier studies [8,10,25]. Physically ACs were obtained at two different holding times at the temperature of 800 °C (1 and 3 h) and denoted as *AC-CO2-X*, where *X* corresponds to the holding time in hours.

For chemical activation with KOH, two methods were used: (1) wet impregnation and (2) dry mixture. For wet impregnation, 10 g of biochar was added to 44.5 or 89 mL of a KOH aqueous solution (4 M) leading to KOH/biochar mass ratios of 1:1 and 2:1, respectively. These ratios were selected on the basis of findings from earlier studies, which revealed that using relatively high KOH/precursor mass ratios (e.g., ratios higher than 2) led to activated carbons with lower ultra-micropore volumes [14,27]. After soaking and filtrating, the resulting mixtures were firstly washed with an aqueous solution of H_2SO_4 (1 M) to remove the intercalated K compounds (e.g., K_2CO_3) and then washed with deionized water until the pH of the eluate became neutral. Finally, the samples (after drying at 110 °C overnight in a conventional oven) were heated under N_2 (100 mL min^{-1} STP) to 600 or 700 °C (holding time at the final temperature = 60 min) in the same fixed-bed quartz reactor mentioned above at an average heating rate of 10 °C min^{-1}. For the dry mixture method, 10 g of biochar was physically mixed with KOH (particle size lower than 1.5 mm) in an agate mortar at two KOH/biochar mass ratios (2:1 and 5:1). The resulting mixtures were then heated under the

same conditions described above for the wet impregnation method. Chemically ACs are denoted as *AC-KOH-X-Y-Z*, where *X* corresponds to the impregnation method used (*W* for wet impregnation, *D* for dry mixture), *Y* is the mass of KOH per mass unit of biochar, and *Z* denotes the final temperature reached during heating in °C.

In addition to the physically or chemically ACs, all of them prepared from vine shoots-derived biochars obtained by atmospheric slow pyrolysis under a N_2 environment at a peak temperature of 600 °C, the performance for CO_2 adsorption of other vine-shoots derived carbons was also investigated. These additional materials were the following: (1) several vine-shoots derived biochars produced using the same pyrolysis device above-described under different operating conditions, and (2) two vine shoots-derived biochars produced by single-step oxidation. The first category of carbon materials is denoted as *BC-X-Y-Z*, where *X* is the pyrolysis environment (N_2 or CO_2), *Y* corresponds to the absolute pressure applied (0.1 or 1.0 MPa), and *Z* is the pyrolysis peak temperature (600 or 800 °C). For the single-step oxidation process, 10 g of vine shoots (with a particle size range of 0.8–3.0 mm) were heated at 10 °C min^{-1} to 650 °C, at atmospheric pressure, using the same early mentioned fixed-bed quartz reactor under a steady flow (100 mL min^{-1} STP) of a gas mixture containing 3% vol. of O_2 in N_2 (balance) [28]. These biochars were obtained at two different holding times at the peak temperature (1 and 3 h) and denoted as *BC-OXI-X*, where *X* corresponds to the holding time in hours. Fig. 1 summarizes the production pathways for all the materials analyzed in the present study.

2.3. Characterization

N_2 adsorption/desorption isotherms at –196 °C were obtained using an ASAP 2020 gas sorption analyzer from Micromeritics (Norcross, GA). Samples (around 120–200 mg) were previously degassed under dynamic vacuum conditions to constant weight at a temperature of 150 °C. Apparent

specific surface areas (S_{BET}) were calculated using the Brunauer–Emmet–Teller (BET) model at small relative pressures (p/p_0 = 0.01–0.15). Total pore volume (V_t) was determined from the specific volume of N_2 adsorbed at a relative pressure of 0.98–0.99. The t-plot method (carbon black STSA thickness equation) was used to estimate the micropore volume (V_{mic}, for pore sizes lower than 2 nm). A Non-Local Density Functional Theory (NLDFT) method assuming slit-pore geometry was used to estimate the Pore Size Distribution (PSD). The mesopore volume (V_{mes}) was then calculated as the difference between the cumulative pore volume for a pore width of 50 nm and V_{mic}.

Ultra-micropore size distributions and the ultra-micropore volume (V_{ultra}, for pore sizes lower than 0.7 nm) of carbons were estimated from their CO_2 adsorption isotherms at 0 °C, which were measured using the same analyzer described above under the same experimental conditions (initial sample mass and degassing step). For this purpose, a Density Functional Theory (DFT) method assuming slit-pore geometry was employed. Given that some adsorbents could contain mainly ultra-micropores (especially the non-activated biochars), S_{BET} values were also determined from the CO_2 adsorption data at 0 °C for an appropriate linear region of the BET plot, which should be selected according to two consistency criteria [29]: (1) the Rouquerol transform must increase with relative pressure for the data range selected, and (2) the *y* intercept of the linear region must be positive to yield a significant value of the *c* parameter ($c > 0$). Recently, Kim et al. [30] have reported that the BET specific surface areas from CO_2 adsorption at 0 °C can be considered as reasonable proxies for highly ultra-microporous materials.

All the necessary calculations from both N_2 and CO_2 adsorption isotherms were performed using the MicroActive software (v. 4.03) supplied by Micromeritics Instrument Corp.

2.4. CO_2 uptake and selectivity

The CO_2 adsorption capacities at 25 and 75 °C at an absolute pressure of 15 kPa were determined from the respective CO_2 adsorption isotherms, which were obtained using the ASAP 2020 gas sorption analyzer at the same experimental conditions with the exception of temperature.

To estimate the apparent selectivity towards CO_2 over N_2, adsorption experiments at atmospheric pressure (under pure CO_2 or N_2) were conducted in a thermogravimetric analyzer (TGA) composed of a MK2 microbalance (precision of 0.1 μg) from CI Precision (UK). Samples (with an initial mass of around 20 mg) were firstly degassed under a steady flow of He (100 mL min^{-1} STP) at 150 °C for 1 h. After cooling to the desired temperature (25 or 75 °C), carrier gas was switched from He to CO_2 or N_2 (100 mL min^{-1} STP).

3. Results and discussion

3.1. Porous properties and CO_2 adsorption capacity at 0 °C

3.1.1. Specific surface area and micropore volume

Table 1 summarizes the textural properties of carbons deduced from both the N_2 adsorption isotherms at –196 °C (see Fig. S1 in Supplementary Data) and CO_2 adsorption isotherms at 0 °C (see Fig. 2). As expected, the non-activated carbons (i.e., biochars) showed a very low N_2 adsorption capacity at –196 °C, due to the fact that the porous structure of these materials is almost entirely composed of ultra-micropores. At cryogenic temperatures, the diffusion rate of the N_2 molecules into ultra-micropores is extremely slow [30]. As a result, the values of S_{BET} determined from the N_2 adsorption isotherm for some biochars became very low. For these biochar samples, the total pore volume (V_t) and the micropore volume (V_{mic}) were unable to be determined using the t-plot method. Hence, these values are indicated as NA in Table 1. For the ACs, however, the values of S_{BET} (538−1671 m^2 g^{-1}) and V_{mic} (0.177−0.587 m^2 g^{-1}) were within the common range reported in the literature for biomass-derived activated carbons [8,10,13,17,31].

As expected, the S_{BET} values determined from the CO_2 adsorption isotherm at 0 °C for non-activated biochars were much higher than those determined from the N_2 adsorption isotherm at –196 °C. Table 1 also reports the Langmuir surface areas (S_L), which were also determined from the CO_2 adsorption isotherms at 0 °C. Given that the range of relative pressures selected for the estimation of both the S_{BET} and S_L values was the same (0.01–0.02), a reasonable agreement between the two models was found. In addition, a linear correlation between S_{BET} and V_{ultra} (*adjusted* R^2 = 0.962) was found for the data pairs corresponding to all biochar samples (BCs). This fact can suggest that the porosity of these samples is exclusively due to ultra-micropores. It should also be noted that S_{BET} and V_{ultra} were not linearly correlated (*adjusted* R^2 = 0.414) when the data corresponding to all ACs were considered.

3.1.2. Ultra-micropore volume

The V_{ultra} values listed in Table 1 were particularly high for all the ACs (0.103–0.148 $cm^3\ g^{-1}$) and the BC-CO2-0.1-800 sample (0.096 $cm^3\ g^{-1}$). In some previous studies, similar or slightly lower ultra-micropore volumes (also estimated using DFT or NLDFT methods) were reported by Hao et al. [8] (0.072–0.128 $cm^3\ g^{-1}$, for several biowaste-derived hydrochars physically activated with CO_2 at 800 °C), Li et al. [14] (0.08–0.15 $cm^3\ g^{-1}$, for rice husk-derived chars chemically activated with KOH at 640–780 °C), and Li et al. [32] (0.079–0.115 $cm^3\ g^{-1}$, for chitosan-derived chars chemically activated with KOH at 600 °C). It should be pointed out that other previously reported ultra-micropore volumes, which were estimated using alternative methods, such as the Horvath-Kawazoe approach (used by Ren et al. [33]) or the procedure based on the Dubinin−Radushkevich equation (used by Yang et al. [9], and Chen et al. [17]), are not directly comparable, since the appropriateness of these estimation techniques was questioned [34]. Fig. 3 shows the ultra-micropore size

distributions, which were determined for selected samples using the DFT method from CO_2 adsorption data at 0 °C.

Another interesting finding is that, for chemically ACs using the wet impregnation method, the highest ultra-micropore volume (and highest CO_2 adsorption capacity at 0 °C and 15 kPa) was obtained for the AC-KOH-W-1-700 sample. This could confirm the fact that higher KOH/biochar ratios can promote the formation of pores with sizes above 0.7 nm. In fact, higher V_{mic} and V_{mes} values are reported in Table 1 for chemically ACs (using the wet impregnation method) at a KOH/biochar mass ratio of 2 compared to those obtained for chemically ACs at the same activation temperature and at a KOH/biochar ratio of 1.

3.1.3. CO_2 uptake capacity at 0 °C

Also from the results shown in Table 1, it can be concluded that the CO_2 adsorption capacities, at 15 kPa and 0 °C, are quite satisfactory for all the ACs developed in the present study. Particularly relevant are the results obtained for the chemically ACs using the wet impregnation method (CO_2 uptakes at 15 kPa ranging from 2.16 to 2.42 mmol g^{-1}) as well as the AC-KOH-D-5-700 sample (2.27 mmol g^{-1}). These values are in the upper range of those reported in previous studies for biomass-derived ACs [8–10,14,17,31,35–37].

Another relevant finding is the similar CO_2 adsorption capacity at 15 kPa and 0 °C observed for the physically ACs (1.79–1.89 mmol g^{-1}) and the BC-N2-0.1-800 sample (1.68 mmol g^{-1}). This fact is particularly interesting, since the production of physically ACs could be done through a single-step process. Regarding the CO_2 uptakes measured for biochars produced at 600 °C, it should be pointed out that the values displayed in Table 1 are relatively high, given the absence of any further activation step at higher temperatures. Unexpectedly, the biochars produced through single-step oxidation at 650 °C exhibited the worst CO_2 uptake capacity at 15 kPa (0.92–1.00 mmol g^{-1}). These

results are substantially lower than those reported by Plaza et al. [28] for biochars produced under the same conditions from almond shells and olive stones (1.80 and 1.65 mmol g^{-1}, respectively). This fact could be due to the dependence of the CO_2 uptake capacity on the biomass precursor, since the development of ultra-micropore volumes can also be affected by the nature of the biomass feedstock.

Fig. 4 displays the linear correlation between the ultra-micropore volume and the CO_2 adsorption capacity for all the adsorbents at 0 °C. It should be highlighted the strong correlation observed for the CO_2 uptake at 15 kPa. This seems to confirm the key role of ultra-micropores in enhancing the CO_2 adsorption at low partial pressures, as was previously stated by Hao et al. [8].

3.2. Temperature-dependent adsorption of CO_2

Fig. 5 shows the CO_2 adsorption isotherms at 25 and 75 °C for selected samples (i.e., the most promising adsorbents according to their performance at 0 °C): the BC-CO2-0.1-800 adsorbent (for its acceptable performance at 0 °C), the two physically ACs, and the best chemically ACs in terms of CO_2 uptake at 0 °C and 15 kPa (the AC-KOH-D-5-700 adsorbent and the four chemically ACs via wet impregnation). At 25 °C, the highest CO_2 adsorption capacity at 15 kPa was 1.35 mmol g^{-1} for the AC-KOH-W-1-700 sample. However, it should be pointed out that the rest of carbons exhibited similar values, all of them within a relatively narrow range of 1.05–1.35 mmol g^{-1}.

Table 2 summarizes the CO_2 uptake capacity at 25 °C recently reported in the literature for some advanced ACs produced from both lignocellulosic and non-lignocellulosic precursors. The highest CO_2 adsorption capacity reported here is similar or higher than that reported in some earlier studies [8,10,17,31,35,36,38], including some adsorbents produced via surface modification pretreatments (such as urea modification for ACs prepared by Chen et al. [17] and preoxidation with H_2O_2 followed by an ammoxidation step used by Guo et al. [35]). Table 2, however, also reports slightly

or appreciably higher CO_2 uptakes for some adsorbents produced from N-doped non-lignocellulosic precursors [33,39] as well as from certain biomass sources (such as rice husks [14], coconut shells [9], pine nut shells [40], and Jujun grass [41]) through pyrolysis or hydrothermal carbonization and subsequent chemical activation with KOH. This fact also suggests that the nature of the precursor plays a key role in determining the performance of the derived AC in terms of CO_2 adsorption capacity, regardless of the presence of absence of nitrogen functionalities on surface. In this sense, the hierarchical porosity development during activation can be strongly conditioned by the textural properties of biomass precursors. In line with this, Deng et al. [40] partially attributed their exceptional results (CO_2 uptake at 25 °C and 15 kPa of 2.00 mmol g^{-1}) to the hard-textural structure of the pine nut shell, which can promote the formation of ultra-micropores in the very narrow range of 0.33–0.40 nm.

For adsorption at 75 °C, the best material in terms of CO_2 uptake at 15 kPa was the AC-CO2-3 sample with a value of 0.465 mmol g^{-1}. A very similar CO_2 adsorption capacity was measured for the AC-CO2-1 sample (0.460 mmol g^{-1}) whereas the rest of carbons exhibited values within the range of 0.321–0.399 mmol g^{-1}. It should be highlighted that Deng et al. [40] reported a CO_2 uptake capacity of around 0.5 mmol g^{-1} at 75 °C and 15 kPa (a very close value to that reported here for physically ACs) for their exceptional pine nut shell-derived ACs. A CO_2 adsorption capacity (at 80 °C and 15 kPa) of around 0.5 mmol g^{-1} was also reported by Hao et al. [37] for a chemically activated carbon (with KOH at a mass ratio KOH/precursor of 2 and at 700 °C) from hydrothermally treated lignin (from eucalyptus). The better performance of our physically ACs at high temperature, as compared to the chemically ACs developed in the present study, could be explained by kinetic reasons, since the time required to reach the equilibrium at temperatures higher than 0 °C is probably much longer than the regular equilibrium interval selected in the ASAP 2020 device (20 s). In this

sense, and as found in Table 1, the higher mesopore volumes for physically ACs, in comparison with the chemically ACs, can enhance the diffusion into micropores and ultra-micropores by shortening diffusion paths.

Deng et al. [40] suggested that the ultra-micropores of ACs responsible for CO_2 adsorption are dependent on the adsorption temperature. More in detail, these authors stated that, under typical flue gas conditions (75 °C and 15 kPa), only the ultra-micropores in the range of 0.33–0.40 nm were effective for CO_2 adsorption. From the ultra-micropore size distributions shown in Fig. 3, however, it seems difficult to detect significant differences in pore volumes for the narrow range of 0.33–0.40 nm. Hence, the variability observed in the present study for the CO_2 adsorption capacity at 75 °C could be mainly explained by differences in the diffusion rate of CO_2 into the ultra-micropores.

The relatively low CO_2 adsorption capacity of the adsorbent produced via a single-step carbonization and activation with CO_2 (BC-CO2-0.1-800) at 25 and 75 °C, compared with that measured for physically ACs, could be explained by differences in the reactor configuration. In this regard, the pyrolysis reactor used in the present study to produce biochars was designed with the aim of maximizing the contact time between biochar and pyrolysis vapors, leading to an additional production of carbon via secondary charring reactions. The deposition of this carbon on the char surface can then lead to partial pore blockage and CO_2 diffusion resistance. This fact can also explain the low total pore volume (V_t) measured for the BC-CO2-0.1-800 sample.

3.3. Apparent selectivity towards CO_2

Despite the fact that the TGA experiments were conducted at an absolute pressure of 101.3 kPa (for both CO_2 and N_2 gases), interesting information regarding the apparent adsorption rate and kinetic selectivity can be extracted from the obtained data. The apparent CO_2-over-N_2 selectivity was calculated as follows:

$$S = \frac{q_{CO_2}}{q_{N_2}} \sigma \quad (1)$$

where q_{CO_2} and q_{N_2} are the uptake capacities (in mmol g^{-1}) at 101.3 kPa after 1 min of CO_2 and N_2, respectively. This time value is within the usual range of gas residence times for the adsorption step in vacuum switch adsorption (VSA) processes [42]. In Eq. (1), the term σ represents the ratio of the CO_2 uptake at 15 kPa to that at 101.3 kPa from the corresponding adsorption isotherm.

It should be highlighted that the apparent selectivity calculated according to Eq. (1), which represents a practical approximation of the selectivity from a kinetic point of view (i.e., continuous-flow breakthrough conditions), cannot be directly compared with those estimated from the single adsorption isotherms and according to the approach based on the ideal adsorbed solution theory (IAST) for binary mixtures [43]. Eq. (1) can lead to conservative estimates of the CO_2-over-N_2 selectivity, since they were calculated from the dynamic adsorption of pure components. In accordance with González et al. [10], the uptake of the weak adsorbate (N_2 in this case) in a multicomponent adsorption system can be significantly lower than that measured during the single-component adsorption. Table 3 summarizes the results obtained for the apparent CO_2-over-N_2 selectivities at 25 and 75 °C and an adsorption time of 1 min (see also Figs. S2 and S3 showing all the dynamic adsorption curves).

From the data shown in Table 3, it can be seen that all the selected adsorbents, with the exception of the AC-KOH-W-2-700 sample, exhibited very high apparent selectivities towards CO_2 at 25 °C (being the highest value of 115 for the AC-CO2-1 sample). González et al. [10] reported a CO_2-over-N_2 selectivity of 33 for the dynamic adsorption at 101.3 kPa and 25 °C (in a fixed-bed adsorption unit) of a binary mixture of CO_2 and N_2 (14% vol. CO_2) onto an almond shell-derived AC. Recently, Ren at al. [33] have measured a selectivity factor of 63 for the dynamic adsorption (in a thermogravimetric analyzer) of a mixture CO_2/N_2 (15% vol. CO_2) at 101.3 kPa and 35 °C onto

a N-doped porous carbon. Interestingly, it should be noted that Ren et al. [33] determined a CO_2-over-N_2 IAST selectivity (i.e., from the static adsorption isotherms of pure components) of only 26 for the same adsorbent at 101.3 kPa and 25 °C.

At 75 °C, however, the apparent selectivity notably decreased for most of our samples, revealing that CO_2 adsorption is more temperature-dependent than N_2 adsorption [44]. At this temperature, the highest factors were obtained for the BC-CO2-0.1-800 and AC-KOH-W-1-700 samples (56.8 and 47.3, respectively). The low selectivity factors obtained for the AC-KOH-W-2-700 adsorbent at both temperatures could be due to its lower V_{ultra}/V_{mic} ratio (see Table 1).

On the other hand, it should be noted that the physically ACs exhibited faster CO_2 adsorption rates than chemically ACs, especially a 75 °C (see Table 3 and Figs. S2 and S3). As has been stated before, the more hierarchical pore structure of physically ACs can lead to a higher diffusion rate of CO_2.

In any case, it must be emphasized that the apparent selectivities reported in Table 3 should be considered as estimates of the real selectivity for a multicomponent gas stream. The accuracy of Eq. (1) has to be confirmed in further experimental studies (e.g., adsorption/desorption cycles in a fixed-bed column).

3.4. Heat of adsorption

To further understand the adsorption process, it is important to estimate the isosteric heat of adsorption, which is an indicator of the interaction between the adsorbate molecules and the surface of the adsorbent [45]. The isosteric heats of adsorption (Q_{st}) at a specific adsorbate loading (q) were calculated from the CO_2 adsorption isotherms at 0, 25 and 75 °C using the Clasius-Clapeyron equation (and assuming no temperature dependence of Q_{st}) [1,8,40,45]:

$$\frac{-Q_{st}}{R} = \left(\frac{\partial \ln p}{\partial T^{-1}}\right)_q \quad (2)$$

The adsorption isotherms were previously fitted to the Tóth model to obtain the values of pressure at a given value of CO_2 loading. The procedure followed to estimate the Q_{st} values, which are shown in Fig. 6, is detailed in Supplementary Data.

From Fig. 6, it can be seen that the isosteric heats of adsorption were in the range of 24.5–29.7 kJ mol^{-1} at low uptake of CO_2. These values are similar or slightly lower than those reported in previous studies for porous carbons [1,8,17,18,33,35,37,38,46]. For physically ACs as well as the adsorbent produced by a single-step method (BC-CO2-0.1-800), the isosteric heats decreased with an increase in surface coverage. This variation in Q_{st} can be related to an energetically heterogeneous surface [8,11,39]. At the beginning of the adsorption, the higher values of Q_{st} can be attributed to the filling of ultra-micropores, while the lower values of Q_{st} with the increase in the surface coverage can be explained by weaker interactions of confined CO_2 in larger pores. In any case, the observed decrease in Q_{st} with CO_2 uptake is notably lower than those reported in previous studies for N-doped ACs [17,38,39]. The AC-CO2-1 sample exhibited a considerably lower heat of adsorption, suggesting that this AC will require the lowest amount of energy during its regeneration. For chemically ACs, however, the isosteric heats of adsorption remained almost constant irrespective of the surface coverage. This suggests that the adsorption can occur in more homogeneous surfaces. In fact, and as can be seen in Table S2, the fitted values of the parameter *t* in the Tóth equation (which is related to the degree of surface heterogeneity [47]; with values trending to 1 for homogeneous surfaces) were substantially higher for chemically ACs compared to those estimated for the rest of carbons.

4. Conclusions

On the basis of the results discussed above, it can be concluded that vine shoots-derived biochar is an excellent low-cost precursor of ACs for CO_2 adsorption in postcombustion conditions. Exclusively in terms of adsorption capacity at 25 °C and at an absolute pressure of 15 kPa, the chemically ACs using KOH (especially the AC-KOH-W-1-700 sample) exhibited a better performance than the physically ACs. Nevertheless, when we analyze the potential suitability of using vine shoots-derived ACs for CO_2 capture in postcombustion, the physically activated carbon AC-CO2-1 appears as the most promising option in the present study, due to its higher CO_2 uptake capacity and adsorption rate at relatively high temperature (75 °C), its appropriate selectivity at this temperature, and its apparently low energy demand for regeneration. In addition, the physical activation with CO_2 is more feasible at industrial scale than the chemical activation using corrosive alkalis. The findings from this study are thus encouraging, since they open the doors to further studies on developing sustainable vine shoots-derived ACs for CO_2 capture in postcombustion and other interesting applications, such as biogas upgrading and H_2 purification.

Acknowledgements

The authors wish to acknowledge financial support from the Spanish MINECO-DGI (Project ENE2013-47880-C3-1-R). JJM also express his gratitude to the Aragon Government (GPT group) and the European Social Fund for additional financial support.

Appendix A. Supplementary data

Proximate, elemental and XRF analyses of vine shoots; N_2 adsorption isotherms (at –196 °C) of biochars, physically ACs and chemically ACs with KOH; TGA adsorption curves of CO_2 and N_2 at 101.3 kPa and two temperatures (25 and 75 °C); and description of the method used to estimate the isosteric heats of adsorption.

References

[1] M. Yang, L. Guo, G. Hu, X. Hu, J. Chen, S. Shen, W. Dai, M. Fan, Adsorption of CO2 by Petroleum Coke Nitrogen-Doped Porous Carbons Synthesized by Combining Ammoxidation with KOH Activation, Ind. Eng. Chem. Res. 55 (2016) 757–765.

[2] A.E. Creamer, B. Gao, Carbon-Based Adsorbents for Postcombustion CO2 Capture: A Critical Review, Environ. Sci. Technol. 50 (2016) 7276–7289.

[3] J. Baxter, Z. Bian, G. Chen, D. Danielson, M.S. Dresselhaus, A.G. Fedorov, T.S. Fisher, C.W. Jones, E. Maginn, U. Kortshagen, A. Manthiram, A. Nozik, D.R. Rolison, T. Sands, L. Shi, D. Sholl, Y. Wu, Nanoscale design to enable the revolution in renewable energy, Energy Environ. Sci. 2 (2009) 559–588.

[4] M.R. Hudson, W.L. Queen, J.A. Mason, D.W. Fickel, R.F. Lobo, C.M. Brown, Unconventional, Highly Selective CO2 Adsorption in Zeolite SSZ-13, J. Am. Chem. Soc. 134 (2012) 1970–1973.

[5] A.E. Creamer, B. Gao, S. Wang, Carbon dioxide capture using various metal oxyhydroxide–biochar composites, Chem. Eng. J. 283 (2016) 826–832.

[6] A. Silvestre-Albero, J. Silvestre-Albero, M. Martínez-Escandell, F. Rodríguez-Reinoso, Micro/Mesoporous Activated Carbons Derived from Polyaniline: Promising Candidates for

CO2 Adsorption, Ind. Eng. Chem. Res. 53 (2014) 15398–15405.

[7] T.M. McDonald, J.A. Mason, X. Kong, E.D. Bloch, D. Gygi, A. Dani, V. Crocella, F. Giordanino, S.O. Odoh, W.S. Drisdell, B. Vlaisavljevich, A.L. Dzubak, R. Poloni, S.K. Schnell, N. Planas, K. Lee, T. Pascal, L.F. Wan, D. Prendergast, J.B. Neaton, B. Smit, J.B. Kortright, L. Gagliardi, S. Bordiga, J.A. Reimer, J.R. Long, Cooperative insertion of CO2 in diamine-appended metal-organic frameworks, Nature 519 (2015) 303–308.

[8] W. Hao, E. Björkman, M. Lilliestråle, N. Hedin, Activated carbons prepared from hydrothermally carbonized waste biomass used as adsorbents for CO2, Appl. Energy 112 (2013) 526–532.

[9] J. Yang, L. Yue, X. Hu, L. Wang, Y. Zhao, Y. Lin, Y. Sun, H. DaCosta, L. Guo, Efficient CO2 Capture by Porous Carbons Derived from Coconut Shell, Energy Fuels 31 (2017) 4287–4293.

[10] A.S. González, M.G. Plaza, F. Rubiera, C. Pevida, Sustainable biomass-based carbon adsorbents for post-combustion CO2 capture, Chem. Eng. J. 230 (2013) 456–465.

[11] A. Heidari, H. Younesi, A. Rashidi, A.A. Ghoreyshi, Evaluation of CO2 adsorption with eucalyptus wood based activated carbon modified by ammonia solution through heat treatment, Chem. Eng. J. 254 (2014) 503–513.

[12] M. Sevilla, A.B. Fuertes, Sustainable porous carbons with a superior performance for CO2 capture, Energy Environ. Sci. 4 (2011) 1765–1771.

[13] S. Shahkarami, A.K. Dalai, J. Soltan, Y. Hu, D. Wang, Selective CO2 Capture by Activated Carbons: Evaluation of the Effects of Precursors and Pyrolysis Process, Energy Fuels 29 (2015) 7433–7440.

[14] D. Li, T. Ma, R. Zhang, Y. Tian, Y. Qiao, Preparation of porous carbons with high low-

pressure CO2 uptake by KOH activation of rice husk char, Fuel 139 (2015) 68–70.

[15] O. Cheung, N. Hedin, Zeolites and related sorbents with narrow pores for CO2 separation from flue gas, RSC Adv. 4 (2014) 14480–14494.

[16] Y. Zhao, X. Liu, Y. Han, Microporous carbonaceous adsorbents for CO2 separation via selective adsorption, RSC Adv. 5 (2015) 30310–30330.

[17] J. Chen, J. Yang, G. Hu, X. Hu, Z. Li, S. Shen, M. Radosz, M. Fan, Enhanced CO2 Capture Capacity of Nitrogen-Doped Biomass-Derived Porous Carbons, ACS Sustain. Chem. Eng. 4 (2016) 1439–1445.

[18] B. Adeniran, R. Mokaya, Is N-Doping in Porous Carbons Beneficial for CO2 Storage? Experimental Demonstration of the Relative Effects of Pore Size and N-Doping, Chem. Mater. 28 (2016) 994–1001.

[19] M. Sevilla, J.B. Parra, A.B. Fuertes, Assessment of the Role of Micropore Size and N-Doping in CO2 Capture by Porous Carbons, ACS Appl. Mater. Interfaces 5 (2013) 6360–6368.

[20] K. V Kumar, K. Preuss, L. Lu, Z.X. Guo, M.M. Titirici, Effect of Nitrogen Doping on the CO2 Adsorption Behavior in Nanoporous Carbon Structures: A Molecular Simulation Study, J. Phys. Chem. C 119 (2015) 22310–22321.

[21] Spanish Ministry of Agriculture (MAGRAMA), Survey of Surface Areas and Crop Yields (ESYRCE). http://www.mapama.gob.es/es/estadistica/temas/estadisticas-agrarias/agricultura/esyrce/, 2016 (accessed 13 September 2017).

[22] M. Azuara, E. Sáiz, J.A. Manso, F.J. García-Ramos, J.J. Manyà, Study on the effects of using a carbon dioxide atmosphere on the properties of vine shoots-derived biochar, J. Anal. Appl. Pyrolysis 124 (2017) 719–725.

[23] B. Corcho-Corral, M. Olivares-Marín, E. Valdes-Sánchez, C. Fernández-González, A.

Macías-García, V. Gómez-Serrano, Development of Activated Carbon Using Vine Shoots (Vitis Vinifera) and Its Use for Wine Treatment, J. Agric. Food Chem. 53 (2005) 644–650.

[24] A. Barroso-Bogeat, M. Alexandre-Franco, C. Fernández-González, A. Macías-García, V. Gómez-Serrano, Temperature dependence of the electrical conductivity of activated carbons prepared from vine shoots by physical and chemical activation methods, Microporous Mesoporous Mater. 209 (2015) 90–98.

[25] J.M.V. Nabais, C. Laginhas, P.J.M. Carrott, M.M.L.R. Carrott, Thermal conversion of a novel biomass agricultural residue (vine shoots) into activated carbon using activation with CO2, J. Anal. Appl. Pyrolysis 87 (2010) 8–13.

[26] J.J. Manyà, D. Alvira, M. Azuara, D. Bernin, N. Hedin, Effects of Pressure and the Addition of a Rejected Material from Municipal Waste Composting on the Pyrolysis of Two-Phase Olive Mill Waste, Energy Fuels 30 (2016) 8055–8064.

[27] S.-Y. Lee, H.-M. Yoo, S.W. Park, S. Hee Park, Y.S. Oh, K.Y. Rhee, S.-J. Park, Preparation and characterization of pitch-based nanoporous carbons for improving CO2 capture, J. Solid State Chem. 215 (2014) 201–205.

[28] M.G. Plaza, A.S. González, J.J. Pis, F. Rubiera, C. Pevida, Production of microporous biochars by single-step oxidation: Effect of activation conditions on CO2 capture, Appl. Energy 114 (2014) 551–562.

[29] J. Rouquerol, P. Llewellyn, F. Rouquerol, Is the bet equation applicable to microporous adsorbents?, Stud. Surf. Sci. Catal. 160 (2007) 49–56.

[30] K.C. Kim, T.-U. Yoon, Y.-S. Bae, Applicability of using CO2 adsorption isotherms to determine BET surface areas of microporous materials, Microporous Mesoporous Mater. 224 (2016) 294–301.

[31] G.K. Parshetti, S. Chowdhury, R. Balasubramanian, Biomass derived low-cost microporous adsorbents for efficient CO2 capture, Fuel 148 (2015) 246–254.

[32] D. Li, J. Zhou, Z. Zhang, L. Li, Y. Tian, Y. Lu, Y. Qiao, J. Li, L. Wen, Improving low-pressure CO2 capture performance of N-doped active carbons by adjusting flow rate of protective gas during alkali activation, Carbon 114 (2017) 496–503.

[33] X. Ren, H. Li, J. Chen, L. Wei, A. Modak, H. Yang, Q. Yang, N-doped porous carbons with exceptionally high CO2 selectivity for CO2 capture, Carbon 114 (2017) 473–481.

[34] M. Kruk, M. Jaroniec, J. Choma, Comparative analysis of simple and advanced sorption methods for assessment of microporosity in activated carbons, Carbon 36 (1998) 1447–1458.

[35] L. Guo, J. Yang, G. Hu, X. Hu, L. Wang, Y. Dong, H. DaCosta, M. Fan, Role of Hydrogen Peroxide Preoxidizing on CO2 Adsorption of Nitrogen-Doped Carbons Produced from Coconut Shell, ACS Sustain. Chem. Eng. 4 (2016) 2806–2813.

[36] J. Serafin, U. Narkiewicz, A.W. Morawski, R.J. Wróbel, B. Michalkiewicz, Highly microporous activated carbons from biomass for CO2 capture and effective micropores at different conditions, J. CO2 Util. 18 (2017) 73–79.

[37] W. Hao, F. Björnerbäck, Y. Trushkina, M. Oregui Bengoechea, G. Salazar-Alvarez, T. Barth, N. Hedin, High-Performance Magnetic Activated Carbon from Solid Waste from Lignin Conversion Processes. 1. Their Use As Adsorbents for CO2, ACS Sustain. Chem. Eng. 5 (2017) 3087–3095.

[38] H. Cong, M. Zhang, Y. Chen, K. Chen, Y. Hao, Y. Zhao, L. Feng, Highly selective CO2 capture by nitrogen enriched porous carbons, Carbon 92 (2015) 297–304.

[39] G. Sethia, A. Sayari, Comprehensive study of ultra-microporous nitrogen-doped activated carbon for CO2 capture, Carbon 93 (2015) 68–80.

[40] S. Deng, H. Wei, T. Chen, B. Wang, J. Huang, G. Yu, Superior CO2 adsorption on pine nut shell-derived activated carbons and the effective micropores at different temperatures, Chem. Eng. J. 253 (2014) 46–54.

[41] H.M. Coromina, D.A. Walsh, R. Mokaya, Biomass-derived activated carbon with simultaneously enhanced CO2 uptake for both pre and post combustion capture applications, J. Mater. Chem. A. 4 (2016) 280–289.

[42] G.N. Nikolaidis, E.S. Kikkinides, M.C. Georgiadis, Modelling and Optimization of Pressure Swing Adsorption (PSA) Processes for Post-combustion CO2 Capture from Flue Gas, in: A.I. Papadopoulos, P. Seferlis (Eds.), Process Systems and Materials for CO2 Capture, JohnWiley & Sons, Hoboken (NJ), 2017, pp. 343-369.

[43] Y. Chen, D. Lv, J. Wu, J. Xiao, H. Xi, Q. Xia, Z. Li, A new MOF-505@GO composite with high selectivity for CO2/CH4 and CO2/N2 separation, Chem. Eng. J. 308 (2017) 1065–1072.

[44] C. Landaverde-Alvarado, A.J. Morris, S.M. Martin, Gas sorption and kinetics of CO2 sorption and transport in a polymorphic microporous MOF with open Zn (II) coordination sites, J. CO2 Util. 19 (2017) 40–48.

[45] M.S. Shafeeyan, W.M.A.W. Daud, A. Shamiri, N. Aghamohammadi, Adsorption equilibrium of carbon dioxide on ammonia-modified activated carbon, Chem. Eng. Res. Des. 104 (2015) 42–52.

[46] E. Jang, S.W. Choi, S.-M. Hong, S. Shin, K.B. Lee, Development of a cost-effective CO2 adsorbent from petroleum coke via KOH activation, Appl. Surf. Sci. 429 (2018) 62–71.

[47] S. Chowdhury, R. Balasubramanian, Three-Dimensional Graphene-Based Porous Adsorbents for Postcombustion CO2 Capture, Ind. Eng. Chem. Res. 55 (2016) 7906–7916.

Table 1

Textural properties and CO_2 uptake (at 0 °C) of the vine shoots-derived carbons.

Sample	Apparent specific surface area ($m^2\ g^{-1}$)			Specific pore volume ($cm^3\ g^{-1}$)				CO_2 uptake at 0 °C (mmol g^{-1})	
	S_{BET}[a]	S_{BET}[b]	S_L[b]	V_t	V_{mic}	V_{mes}	V_{ultra}	15 kPa	101.3 kPa
BC-N2-0.1-600	1.91	228	242	NA	NA	NA	0.062	1.03	1.94
BC-N2-1.0-600	1.24	244	260	NA	NA	NA	0.069	1.16	2.11
BC-CO2-0.1-600	2.48	252	270	NA	NA	NA	0.070	1.18	2.18
BC-CO2-1.0-600	46.3	254	273	NA	NA	NA	0.072	1.20	2.21
BC-CO2-0.1-800	374	439	467	0.186	0.112	0.069	0.096	1.68	3.45
BC-OXI-1	32.9	205	160	NA	NA	NA	0.060	0.92	1.50
BC-OXI-3	35.7	194	206	NA	NA	NA	0.062	1.00	1.53
AC-CO2-1	593	426	455	0.261	0.181	0.053	0.103	1.79	3.49
AC-CO2-3	767	526	564	0.374	0.245	0.049	0.107	1.89	4.07
AC-KOH-D-2-600	538	447	469	0.236	0.177	0.035	0.112	1.76	3.19
AC-KOH-D-2-700	1032	722	768	0.489	0.348	0.036	0.120	1.92	4.38
AC-KOH-D-5-600	864	591	625	0.405	0.281	0.042	0.110	1.78	3.74
AC-KOH-D-5-700	1439	861	946	0.674	0.493	0.020	0.135	2.27	6.08
AC-KOH-W-1-600	704	495	533	0.291	0.242	0.008	0.131	2.16	4.16
AC-KOH-W-1-700	1101	678	736	0.541	0.377	0.016	0.148	2.42	5.36
AC-KOH-W-2-600	1305	849	932	0.534	0.451	0.017	0.135	2.25	6.04
AC-KOH-W-2-700	1671	726	781	0.670	0.587	0.031	0.135	2.25	5.40

[a] calculated from N_2 adsorption data a –196 °C.

[b] calculated from CO_2 adsorption data a 0 °C.

Table 2

Some CO_2 uptakes at 25 °C and 15 kPa reported in literature for porous carbons derived from different precursors.

Reference	Highest CO_2 uptake reported (mmol g^{-1})	Precursor[c]	Preparation method
Hao et al. [8]	1.10	HTC chars from **grass cuttings**	Physical activation with CO_2 at 800 °C
Li et al. [14]	1.55	Pyrolyzed **rice husks** at 520 °C under N_2	Chemical activation with KOH: wet impregnation at a mass ratio of 1:1 and subsequent heating under N_2 at 710 °C
Ren et al. [33]	1.60	Chemically synthetized polyindole nanospheres	Chemical activation with KOH: wet impregnation at a KOH/precursor mass ratio of 2 and subsequent heating under N_2 at 600 °C
Yang et al. [9]	1.45	Pyrolyzed **coconut shells** at 500 °C under N_2	Chemical activation with KOH: wet impregnation at a mass ratio of 1:1 and subsequent heating under N_2 at 600 °C
Chen et al. [17]	1.40	Pyrolyzed **coconut shells** at 500 °C under N_2	Modification of the precursor by urea (a mixture at a mass ratio of 1:1 was heated in air at 320 °C) and chemical activation of the resulting sample with KOH (wet impregnation at a KOH/precursor mass ratio of 3 and subsequent heating under N_2 at 650 °C)
Cong et al. [38]	1.30	Melamine-doped phenolic-resins (at a melamine/resorcinol mass ratio of 3)	Chemically activation with KOH: wet impregnation at a KOH/precursor mass ratio of 0.25 and subsequent heating under N_2 at 500 °C
Sethia and Sayari [39]	1.70	Pyrolized 1,3-bis(cynomethyl imidazolium) chloride at 400 °C under N_2	Chemically activation with KOH: dry mixture at a KOH/precursor mass ratio of 1.5 and subsequent heating under N_2 at 600 °C
Deng et al. [40]	2.00	Pyrolyzed **pine nut shells** at 500 °C under N_2	Chemically activation with KOH: dry mixture at a KOH/precursor mass ratio of 2 and subsequent heating under N_2 at 700 °C
González et al. [10]	1.10	**Almond shells**	Single-step activation with CO_2 at 800 °C
Guo et al. [35]	1.35	Pyrolyzed **coconut shells** at 500 °C under N_2	Preoxidation with H_2O_2 followed by ammoxidation (by a mixture of ammonia and air at the ratio of 1:10 at 350 °C for 5 h). The resulting samples were then activated with KOH (wet impregnation at a mass ratio of 1:1 and subsequent heating under N_2 at 600 °C)
Parshetti et al. [31]	1.20	HTC chars from **empty fruit brunch** at 350 °C	Chemically activation with KOH: wet impregnation at a KOH/precursor mass ratio of 5 and subsequent heating under N_2 at 800 °C
Serafin et al. [36]	1.25	**Pomegranate peels**	Single-step activation with KOH: wet impregnation at a mass ratio of 1:1 and subsequent heating under N_2 at 700 °C
Coromina et al. [41]	1.50	HTC chars from **Jujun grass** at 350 °C	Chemically activation with KOH: dry mixture at a KOH/precursor mass ratio of 2 and subsequent heating under N_2 at 700 °C

[c] Sustainable lignocellulosic precursors are given in bold.

Table 3

Apparent CO_2-over-N_2 selectivities and CO_2 uptakes at 25 and 75 °C and an absolute pressure of 101.3 kPa deduced from the TGA adsorption tests.

Sample	25 °C			75 °C		
	CO_2 uptake after 1 min (mmol g^{-1})	Percentage of CO_2 adsorbed (%)[d]	Apparent selectivity (molar basis)	CO_2 uptake after 1 min (mmol g^{-1})	Percentage of CO_2 adsorbed (%)[d]	Apparent selectivity (molar basis)
BC-CO2-0.1-800	1.10	64.4	55.2	0.127	47.7	56.8
AC-CO2-1	1.52	76.5	115	0.299	86.2	21.3
AC-CO2-3	1.58	69.0	68.5	0.299	79.5	13.4
AC-KOH-D-5-700	1.98	58.8	56.8	0.131	42.8	14.8
AC-KOH-W-1-600	1.85	64.4	145	0.194	43.4	19.7
AC-KOH-W-1-700	1.93	68.0	42.3	0.213	32.8	47.3
AC-KOH-W-2-600	1.21	44.2	72.6	0.108	25.8	35.4
AC-KOH-W-2-700	2.46	83.7	8.50	0.168	32.2	5.12

[d] Ratio [(uptake of CO_2 after 1 min) / (uptake of CO_2 after 10 min)] in %.

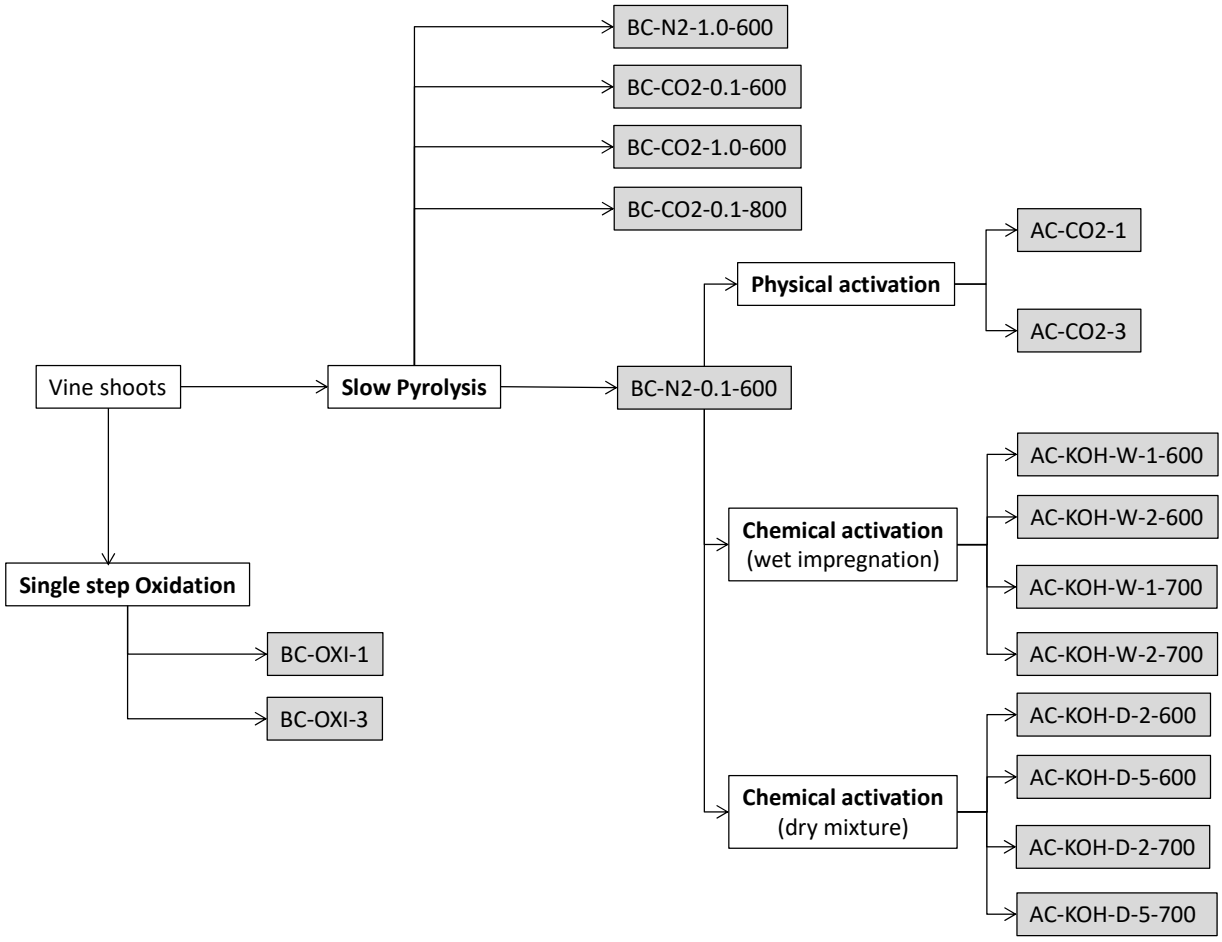

Fig. 1. Graphical scheme of the production pathways for all the vine shoots-derived adsorbents investigated in the present study.

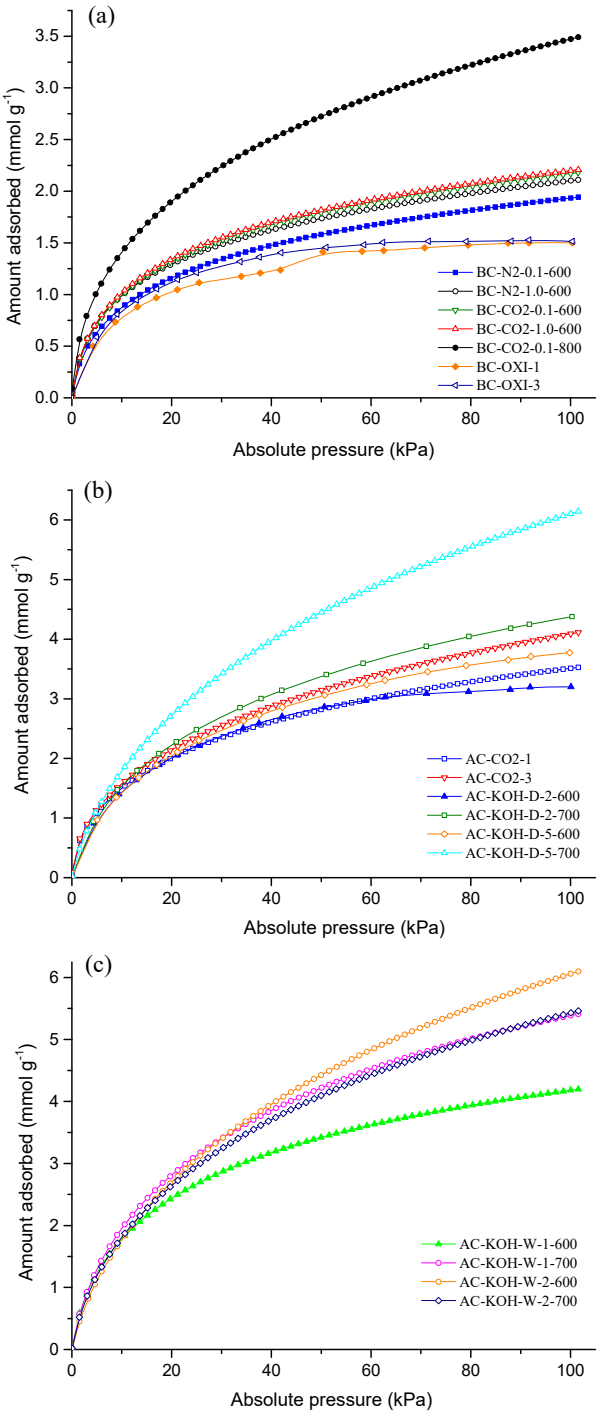

Fig. 2. CO_2 adsorption isotherms (at 0 °C) for (a) biochars, (b) ACs physically activated and chemically activated with KOH using the dry mixture method, and (c) ACs chemically activated with KOH using the wet impregnation method.

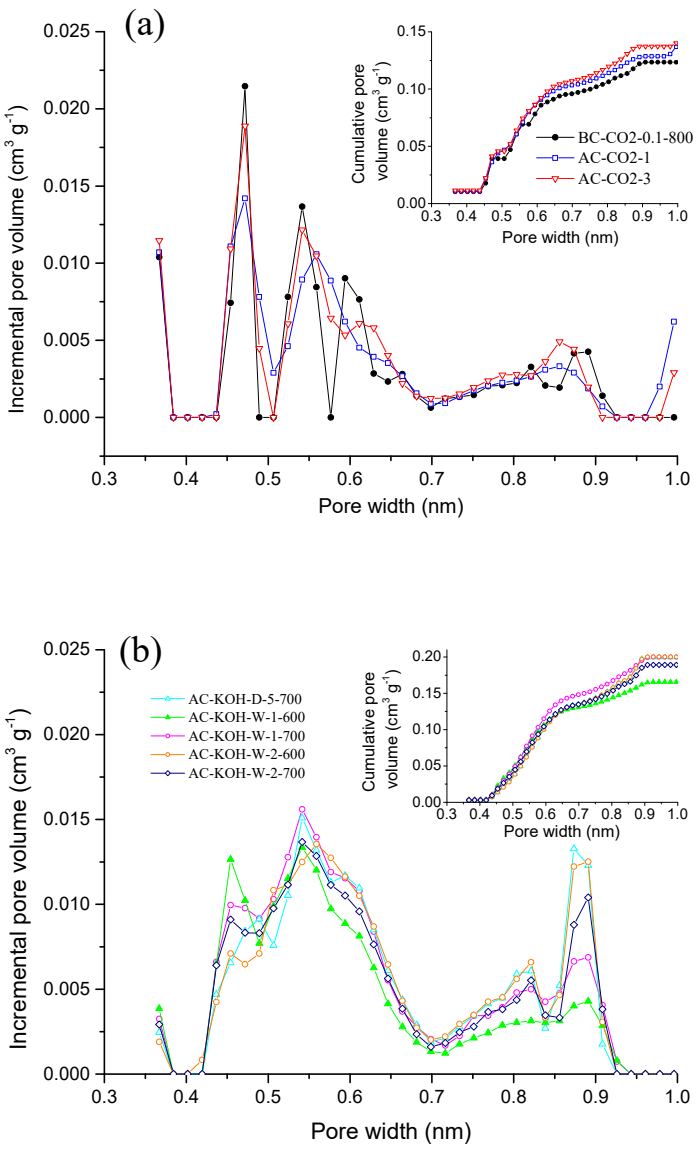

Fig. 3. Ultra-micropore size distributions for (a) physically ACs and the BC-CO2-0.1-800 sample and, (b) chemically ACs with KOH.

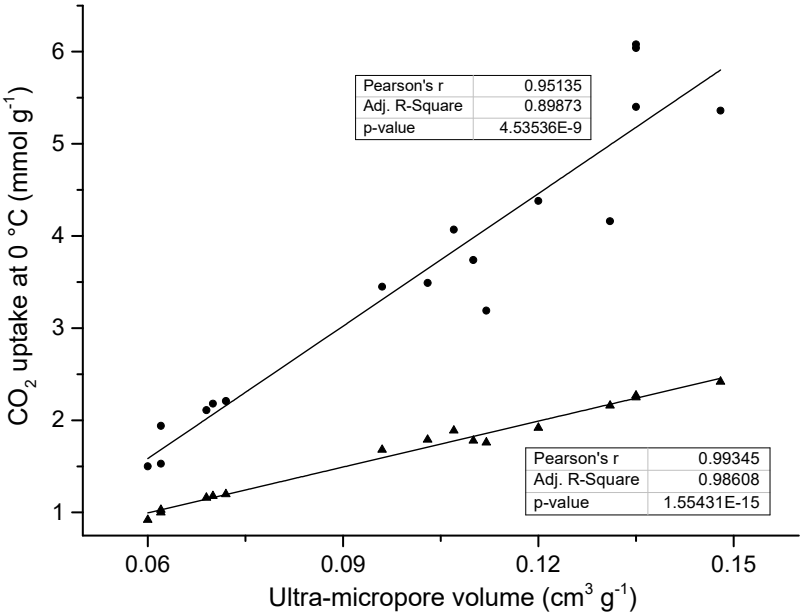

Fig. 4. Linear correlation between the ultra-micropore volume and the CO_2 uptake capacity at 0 °C and CO_2 pressures of 15 kPa (triangles) and 101.3 kPa (circles).

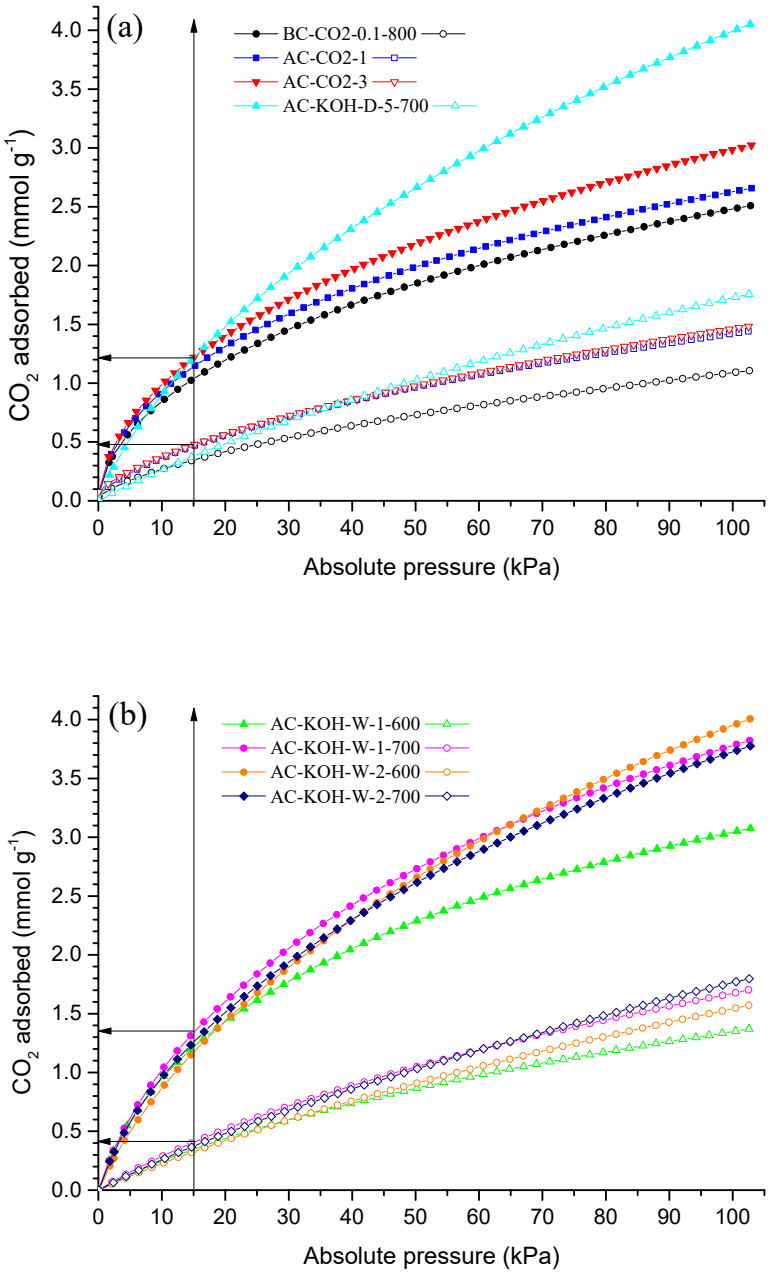

Fig. 5. CO_2 adsorption isotherms at 25 °C (filled symbols) and 75 °C (empty symbols) for the selected biochar samples: (a), BC-CO2-0.1-800, AC-CO2-1, AC-CO2-3, and AC-KOH-D-5-700; and (b), chemically ACs with KOH using the wet impregnation method.

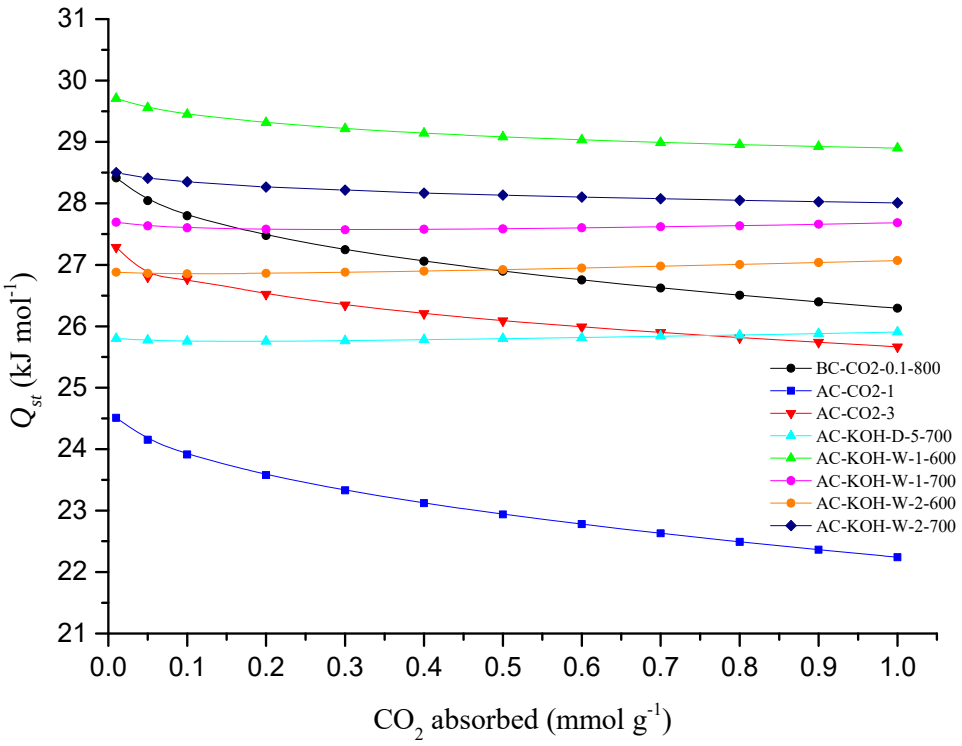

Fig. 6. Isosteric heat of CO_2 adsorption as a function of the amount adsorbed.